Deep–Sea Research II 214 (2024) 105368

Contents lists available at ScienceDirect

Deep-Sea Research Part II

journal homepage: www.elsevier.com/locate/dsr2

Temporal shifts in prokaryotic metabolism in response to organic carbon dynamics in the mesopelagic ocean during an export event in the Southern ocean

Rachel R.-P. Rayne [a,b], Sarah L.C. Giering [b], Manuela Hartmann [b,1], Joost Brandsma [c], Richard D. Sanders [b,2], Claire Evans [b,*]

[a] Ocean and Earth Science, University of Southampton, National Oceanography Centre, Southampton, UK
[b] Ocean BioGeosciences, National Oceanography Centre, Southampton, European Way, Southampton, UK
[c] Henry M. Jackson Foundation for the Advancement of Military Medicine (HJF), 6720A Rockledge Drive, Bethesda, MD, 2081, United States

ARTICLE INFO

Handling Editor: Prof. J Aristegui

Keywords:
Energy limitation
Carbon limitation
Prokaryotic metabolism
Prokaryotic production
Prokaryotic respiration
mesopelagic
Spring bloom
Southern ocean
Biological carbon pump
Growth efficiency
leucine

ABSTRACT

As the major term in downward organic carbon flux attenuation, determining prokaryotic metabolism over depth in the mesopelagic ocean is crucial for constraining the efficiency of the gravitational biological carbon pump (BCP). We hypothesize that the enhancement of particulate organic carbon (POC) concentrations in the mesopelagic twilight zone during export events leads to a temporally dynamic prokaryotic metabolic response, which likely has consequences for the efficiency of the BCP. We tested this hypothesis by making repeated measurements of leucine assimilation and leucine respiration at in situ concentrations over six depths throughout the upper 500 m of the water column during the collapse of a large-scale Southern Ocean spring diatom bloom. Rates of prokaryotic leucine assimilation were used to indicate levels of prokaryotic heterotrophic production, and leucine assimilation efficiency (LAE; the proportion of leucine used for growth versus respiration) was taken as an indicator of prokaryotic growth efficiency. Thus, relative shifts in LAE are indicative of shifts in rates of prokaryotic production relative to respiration. The flux of POC through the oceans' interior led to a dynamic prokaryotic response, characterized by a temporary elevation in mesopelagic prokaryote leucine assimilation rates, LAE and prokaryotic abundance. By the final measurement these changes had already begun to revert, despite POC concentrations still being enriched. As hypothesized, our data revealed distinctions in the phases of the mesopelagic system, likely due to an evolution in bulk prokaryotic metabolic status and the amount and composition of organic matter available. This indicates that estimating ocean carbon sequestration during export events necessitates a time course of measurements throughout the period of POC downward flux. Our findings also revealed distinctions in the ecophysiological prokaryotic responses to substrate regimes between the surface mixed layer and the mesopelagic. Specifically, in the latter in situ leucine concentrations appeared more significant in controlling prokaryote metabolism than POC concentration, and were more closely related to per cell leucine assimilation, than respiration. Whereas, in the mixed layer, the concentration of in situ leucine did not seem to drive rates of its assimilation, rather POC concentration was a strong negative driver of cell specific leucine respiration. These findings are suggestive of stronger levels of energy limitation in the deeper ocean. We surmised that ocean regions with sporadic substrate supply to the mesopelagic are likely to experience stronger energy limitation which favors prokaryotic respiration over production.

1. introduction

The flux of organic matter from the surface to the depths of the ocean forms a significant element of the gravitational biological C pump (BCP), which is a key term in determining Ocean C storage (Eppley and Peterson, 1979; Volk and Hoffert, 1985; Boyd et al., 2019). As

* Corresponding author.
E-mail address: clevans@noc.ac.uk (C. Evans).
[1] Present address: Helmholtz Pioneer Campus, Helmholtz Zentrum München, Munich, Germany.
[2] Present address: Norwegian Research Centre, Bjerknes Centre for Climate Research, Bergen, Norway.

https://doi.org/10.1016/j.dsr2.2024.105368
Received 30 September 2022; Received in revised form 31 January 2024; Accepted 4 February 2024
Available online 10 February 2024

prokaryotic consumption is the dominant process by which the downward flux of organic material is reduced or attenuated (Steinberg et al., 2008; Giering et al., 2014), the levels of prokaryotic metabolic activity over depth will influence the efficiency of the BCP (Cho and Azam, 1988; Kwon et al., 2009). Despite their importance for the Ocean's ability to store C (Cho and Azam, 1988), heterotrophic metabolic rates over the surface to mesopelagic, and particularly how these vary in response to dynamic substrate inputs, are still poorly constrained.

Vertical gradients in the rates of marine prokaryotic heterotrophic production (PHP; (Reinthaler et al., 2010; Manganelli et al., 2009) and respiration (PR), as well as their relative strength (i.e., prokaryotic growth efficiency: PGE=PHP/(PHP + PR)), are thought to be driven largely by the availability of organic matter (Vallino et al., 1996; del Giorgio and Cole, 1998; Eiler et al., 2003). In turn, organic matter availability is likely a function of a number of factors, including its concentration, composition and complexity (Dittmar, et al., 2021), and the metabolic capacity of the prokaryotic community present to consume it (Wu et al., 2018; Ebrahimi et al., 2019; Nguyen et al., 2022). In general, transformation and consumption of organic matter by prokaryotes as matter sinks is thought to lead to an overall downward reduction in substrate concentration and bioavailability (Pomeroy et al., 2007; Jiao et al., 2011). However, during scenarios of variable downward particulate organic carbon (POC) flux the factors influencing prokaryotic metabolism over depth are unlikely to be in steady state, meaning vertical gradients of PHP and PR will be dynamic.

The dynamic factors which determine substrate characteristics and prokaryotic metabolic capacity during scenarios of variable downward POC flux will mainly pertain to the 'activities and interactions' of the organic system. Factors such as particle sinking speed are believed to influence the composition of their associated microbial communities and the nature of organic substrates they supply via leaching to the dissolved phase (Alcolombri, 2021; Ebrahimi et al., 2019). Likewise herbivory leads to compositional changes to organic matter elicited by consumption and excretion (De Corte et al., 2022), including the potential to generate fecal material enriched with microbes originating from the grazers' gut (Maas et al., 2020), and are a function of primary producer accumulation (Tang et al., 2010). Mortality agents such as viruses and bacteriovores are often host/prey specific and density dependent (Wikner and Hagström, 1988; Middelboe, 2000). Thus, the succession of microbial community structure and the shifts to organic matter composition (Wu et al., 2018) that they drive is likely continually evolving under variable organic matter supply. Similarly, the action of fungi metabolizing OM over depth (Raghukumar, 2017) may be subject to thresholds or nonlinear metabolic responses. Furthermore, when considering prokaryotes in the mesopelagic, it is likely that their maintenance energy requirements, relative to growth, are impacted by the episodic nature of substrate supply (Sebastián et al., 2019; Smith Jr et al., 2018; Conte et al., 2001) with consequences for growth efficiency and thus the strength of anabolic versus catabolic metabolism.

We hypothesize that the enhancement of POC concentrations in the mesopelagic twilight zone during export events leads to a temporally dynamic prokaryotic metabolic response, which likely has consequences for the efficiency of the BCP, depending on the phase of this response. The sinking organic flux, and hence the resulting magnitude of shifts in prokaryotic metabolic rates and growth efficiencies over depth, is likely most pronounced at high latitudes, given its association with the intense, seasonal burst of primary production known as the spring bloom. Increasing insolation and stratification traps nutrients above the thermocline, leading to a temporary decoupling between phytoplankton production and loss processes. The resulting accumulation of biomass is eventually terminated by nutrient limitation (Blain et al., 2004; Nielsdóttir et al., 2009), viral infection (Suttle et al., 1990), grazing (Banse, 1994), and sinking (Briggs et al., 2011) causing a temporary enhancement of downward POC flux (Lampitt et al., 2010; Behrenfeld and Boss, 2014; Llort et al., 2015).

We tested our hypothesis by examining profiles of prokaryotic metabolism over six depths in the upper 500 m of the water column during the collapse of a large-scale Southern Ocean spring diatom bloom. Profiles were determined at six time points over the decline of the bloom, which encompassed the initial phase of high biomass in the surface waters and low biomass in the mesopelagic to a final time point, where bloom decline and POC sinking had reversed this biomass distribution.

To constrain dynamics in prokaryotic metabolism we measured leucine assimilation and leucine assimilation efficiency (LAE; the proportion of leucine used for growth versus respiration) as indicators of prokaryotic heterotrophic production (Ducklow and Kirchman, 2000) and prokaryotic growth efficiency respectively. An isotope dilution time series bioassay method was employed (Wright and Hobbie, 1966; Zubkov et al., 2007), which determines in-situ leucine assimilation rates and in-situ leucine concentrations (Zubkov et al., 2007). For measurements below the mixed layer, where ambient leucine concentrations are significantly lower, we devised an adaptation of the bioassay that uses much lower concentrations of leucine, to avoid saturating the prokaryotes and thereby perturbing leucine uptake rates (Giering and Evans, 2022). $A^{14}C$ leucine tracer method (Hill et al., 2013) was used to measure leucine respiration. According to the findings of (Schapira et al., 2012) such leucine uptake based methods yield rates based on the contribution of both free living and particle associated prokaryote metabolism. The rates of, and the ratio between, leucine used for anabolism versus catabolism, was examined alongside changes in POC and ambient leucine concentrations over depth, to determine how the nutritional and energetic status of the prokaryotic community changed over the export event.

2. | methods

We conducted our study during the first Controls Over Mesopelagic Interior Carbon Storage (COMICS) expedition to the Scotia Sea in November to December 2017 aboard the Royal Research Ship (RRS) *Discovery* (cruise DY086; Fig. 1). We made repeated measurements of prokaryotic abundance and metabolism, from six CTD casts approximately every six days. Seawater was collected in 20-L Niskin bottles attached to a stainless steel CTD rosette from six depths, specifically surface (6 m), deep-chlorophyll max (DCM), mixed layer +10 m, mixed layer +100 m, 250 m, and 500 m. Seawater was collected into 9-L acid-cleaned HDPE carboys using acid-cleaned silicon tubing, which were then stored at in situ seawater temperature in the dark until experimental set up.

2.1. | *prokaryotic abundance*

Measurements of prokaryote abundance were carried out by flow cytometry. Seawater samples of 1.6 ml volume were fixed with paraformaldehyde (1% final concentration) for 30 min at room temperature, before flash freezing in liquid nitrogen and storage at minus 80 °C. Prior to analysis samples were defrosted and stained with the SYBR Green I at 1 x 10^{-4} dilution of the commercial stock concentration (10 000x concentrate, Thermo Fisher Scientific). For samples where the stain concentration was insufficient, as indicated by 'smearing' of the community along the green fluorescence axis, the concentration of SYBR Green stain employed was increased to 5 x 10^{-4} dilution of the commercial stock concentration (Marie et al., 1997). An internal standard of fluorescent beads (Fluoresbrite microparticles, Polysciences; (Zubkov and Burkill, 2006) was added before enumeration on BD FACSort™ flow cytometer.

2.2. | *prokaryotic leucine assimilation*

Prokaryotic leucine assimilation was determined by time series dilution bioassay (Hill et al., 2013) using L-[4,5-^{3}H] leucine (specific activity 89.3 Ci mmol^{-1}, Hartmann Analytic). For seawater collected

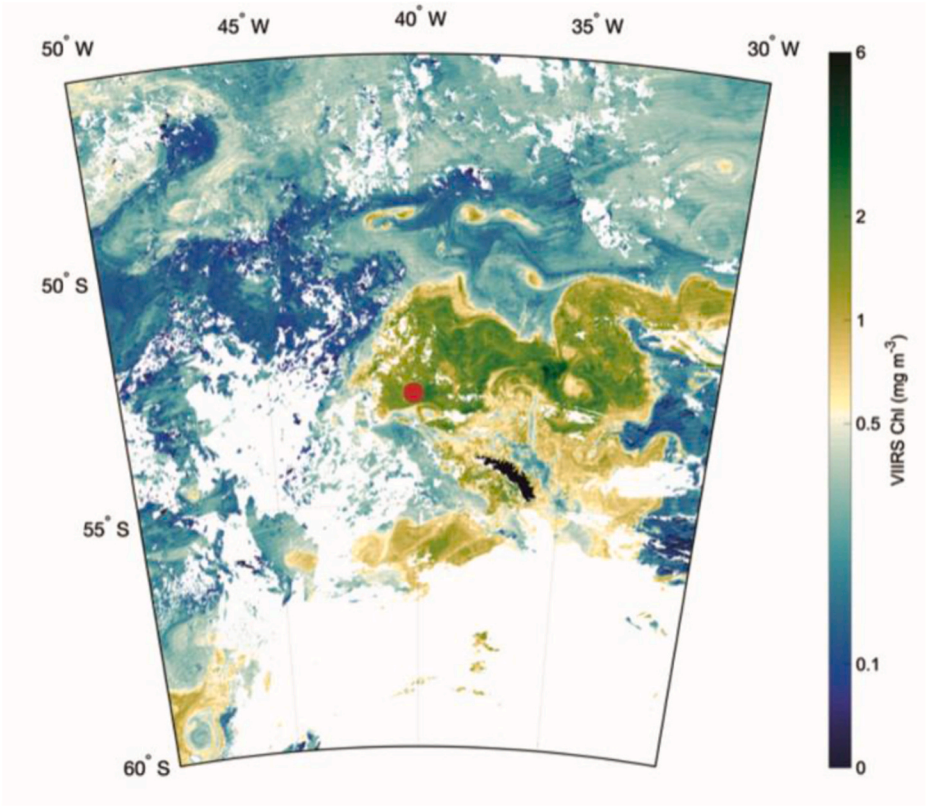

Fig. 1. Satellite derived image of Chlorophyll (green) concentration at the start of the study and the location of the study site (red dot). For more details see Carvalho et al. (this issue).

from the upper, mixed layer of the water column the protocol of Zubkov et al. (2007) was followed. Briefly, ^{3}H-Leucine was preloaded into 2 mL polypropylene crystal-clear microcentrifuge tubes (Starlab, Milton Keynes) so that, when 1.6 ml of seawater was added to start the incubation, a final concentration of ^{3}H-leucine of either 0.2, 0.4, 0.6, 0.8 or 1 nM was achieved. For each leucine concentration incubations were conducted for 10, 20, 30, and 40 min. Bioassays were terminated by adding 80 μL of 20% paraformaldehyde (PFA) to a final concentration of 1%. Samples were fixed for 1 h at room temperature before filtering onto 0.2-μm pore-size polycarbonate filters, which were washed twice with 3 mL of deionised water. The filters were placed into scintillation vials to which 4 mL of scintillation cocktail (Meridian, Gold Star) was added and the radioactivity measured as counts per minute (CPM) by liquid scintillation (Tri-Carb, 3110 TR, PerkinElmer, Beaconsfield, UK).

For seawater collected from below the mixed layer several adaptations were made to the bioassay protocol to ensure that the relatively lower rates of in situ leucine assimilation expected there were accurately measured. To prevent stimulating luxury absorption of leucine (Hill et al., 2013) the concentration series of ^{3}H-Leucine employed was adjusted downwards to: 0.005, 0.01, 0.025, 0.04, and 0.05 nM. To facilitate detection of the radiotracer at lower concentrations resulting from the smaller radionuclide 'spike' and expected lower assimilation rates, we increased the experimental volumes to 30 mL and extended the length of the incubations to 30, 60, 90, and 120 min. These larger volume incubations were terminated by pouring the sample into 50 mL centrifuge tubes preloaded with PFA to make a final concentration of 1%.

The ambient rate of bulk leucine assimilation was calculated as the slope of the linear regression of radioactivity against incubation time and used to calculate a leucine turnover time by dividing the amount of leucine added to a sample by the rate of its uptake per min (Fig. 2; Zubkov et al., 2007). The resulting turnover times were plotted against the corresponding concentration of added leucine and extrapolated using linear regressions, from which an estimate of bulk leucine assimilation rate at ambient concentration was derived from the slope, and the ambient leucine concentration present in the seawater was determined from the x-axis intercept. Errors were calculated by finding the standard error of turnover time given the leucine concentration added for the linear regression. An example of the data produced from the classical and our adapted ^{3}H-leucine time series dilution bioassay is provided in Fig. 2.

2.3. | *prokaryotic leucine respiration*

The rate of ^{14}C-Leucine respiration was determined by adding L-[^{14}C (U)] Leucine (specific activity 328 mCi mmol^{-1}, Hartmann Analytic) to a final concentration of 0.4 nM–70 mL of seawater as previously described by (Hill et al., 2013). Incubations were carried out in 160 mL glass crimp neck serum bottles that had been acid cleaned and rinsed three times with sample water before filling with sample. After the addition of ^{14}C-Leucine spike, the serum bottles were sealed using Teflon-coated silicone septa and crimp caps (Fisher Scientific). Samples were incubated in the dark at 11 °C over a four-point time series ranging between 1 and 18 h. Incubations were terminated by injecting 1 mL of 10% HCl through each septum using a hypodermic needle and syringe. Respiration bottles were bubbled with CO_2-free air for 2 h, and the evolved $^{14}CO_2$ was directed via a hypodermic needle through a perforated lid lined with a wetted GFF into a 20 mL scintillation vial. The $^{14}CO_2$ was trapped in 4 mL of Carbo-Sorb contained within the vial. After the bubbling period 16 mL of scintillation cocktail was added to the $^{14}CO_2$ loaded carbo-sorb and vial capped with an unperforated lid. The radioactivity of samples was measured as counts per minute (CPM) by liquid scintillation counting. ^{14}C-leucine respiration was calculated according to Hill et al. (2013) from the slope of the linear regression line over the incubation time for each addition. Errors were calculated by finding the standard deviation between rates derived between each time

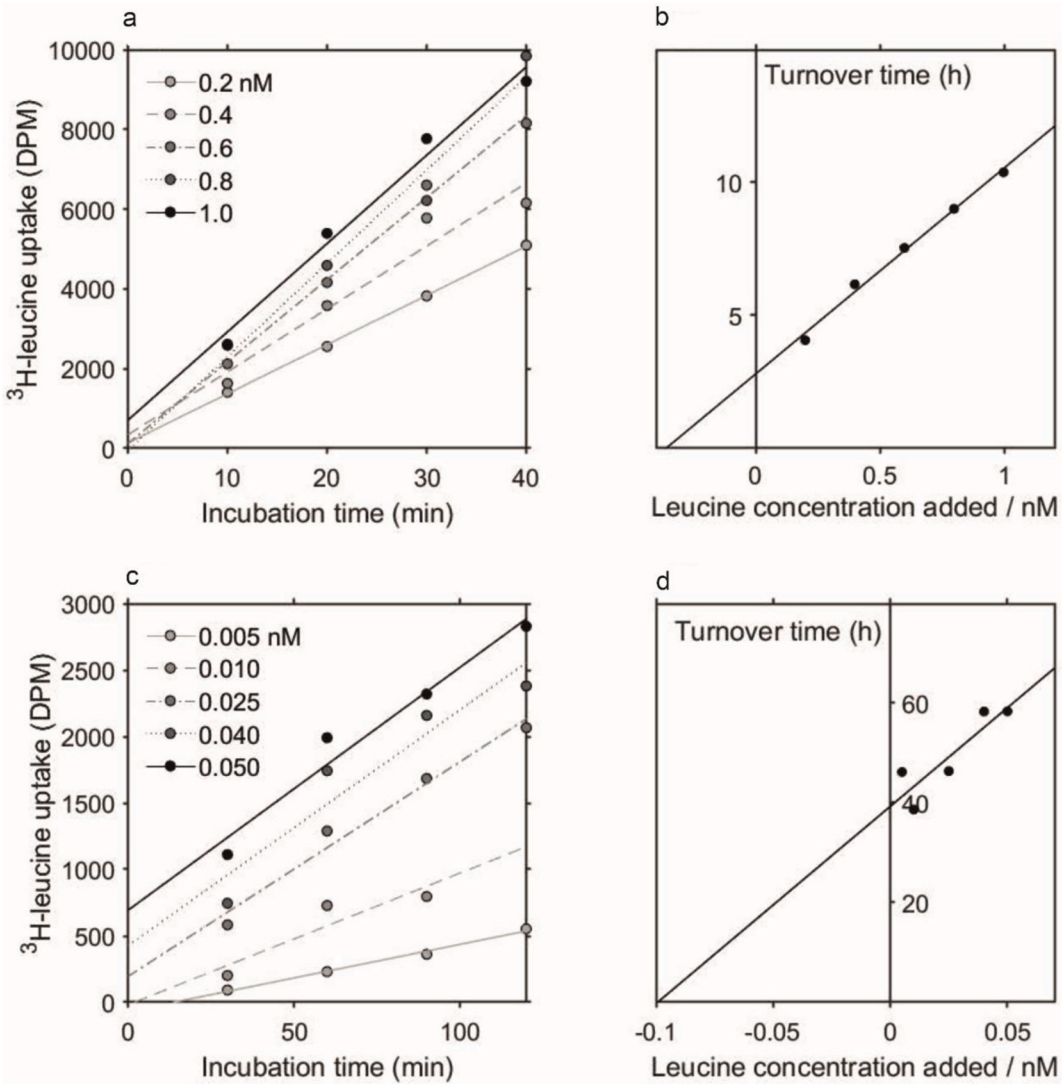

Fig. 2. Time series dilution bioassay estimation of in situ leucine assimilation rates according to (a and b) the standard protocol of Zubkov et al. (2007) and (c and d) the adapted protocol for application at depths below the surface mixed layer. (a and c) The ^{3}H-activity in the prokaryotic biomass resulting from the leucine assimilated over the incubation time series is used to derive a leucine turnover time for each concentration. (b and d) Leucine turnover time are plotted against leucine concentration to derive an ambient leucine assimilation rate from the inverse of the linear regression, and the in situ leucine concentration and turnover time according the x-axis intercept and y-axis intercept respectively. Samples were taken from 6 m on the 30th of November (a and b) and from 500 m on the November 30, 2017 (c and d).

point.

2.4. Leucine assimilation efficiency

The proportion of leucine used for assimilation (LA) versus respiration (LR) known as the Leucine Assimilation Efficiency (LAE = LA/(LA + LR)) was calculated from the results of the time series dilution bioassay in the case of the former (section 2.2) and a fixed concentration incubation experiment in the case of the latter (section 2.3). Given that these methods differ in that assimilation derives an in situ rate from a dilution, time series, whereas the respiration method determines rates of respiration of an added labelled fixed concentration they will contain a bias. To assess the likely difference caused by estimating prokaryotic leucine metabolic rates from a single leucine concentration of 0.4 nM versus using a dilution series to calculate an in situ rate, we derived prokaryotic leucine assimilation from only the 0.4 nM incubation time series, and plotted this against the derived in situ rate (from the concentration series).

2.5. POC concentrations

POC concentrations were determined using measurements made by optical backscattering sensors (at 700 nm) mounted on three gliders which were then calibrated by samples collected from Niskin bottles fitted onto a stainless steel CTD rosette. The glider surveys were conducted as part of the GOCART project (Gauging ocean Organic Carbon fluxes using Autonomous Robotic Technologies) and a full description of the glider mission, capabilities and data are published by Henson et al. (this issue). Concentrations of POC were measured from 12 CTD profiles and at 12 depths (approximately 5, 20, 40, 50, 75, 100, 150, 250, 250, 500, 750 and 1000 m depth). 1000 or 2000 mL of seawater was filtered onto pre-combusted (400 °C, 12 h) GF/F filters (0.7-μm nominal pore size, 25 mm, Whatman), briefly rinsed with MilliQ water to remove salts, dried (50 °C, overnight). On shore, the filters were fumed with HCl (35%, 24 h), dried (50 °C, >24 h), and pelleted in tin disks (Elemental microanalysis). The samples were analysed for POC using a Organic Elemental Analyser. POC calibration was performed at the beginning of each batch using a series of caffeine standards of varying weights (1–5

mg) with known percentage content of carbon. Reference standards were included in each batch after every 10 samples to check the instrument precision (<1%, n = 72, 1 SD) and drift. If needed, a drift correction was applied. All samples were blank corrected. Horizontal POC anomalies were calculated as the difference from the mean POC concentration at each depth.

2.6. | *correlation analysis and representation of the rates*

To explore the relationships between prokaryotic numbers, prokaryotic metabolism and the substrate regime correlations were performed between prokaryotic abundance, prokaryotic assimilation and respiration of leucine, as bulk and per cell values, and ambient leucine and POC concentrations. Correlation matrices were generated in R (v3.6.3) using the ggcorrplot package to determine the Pearson correlation coefficients (r). Correlation were performed for data from the entire water column, and also separately for the mixed layer and mesopelagic. For 2D representation of the data, dates were converted into 'days since November 15, 2017' and depth was binned in 20 m bins in order to generate a grid of equal dimensions (27 ╳ 26). The data was transformed into a spatial point pattern using the spatstat package, Dirichlet regions were calculated using the spatstat's dirichlet function, and each region was assigned the measured metabolic rate.

3. | results

3.1. |*Bloom progression*

The hydrology and biogeochemical conditions over the study period are reported in detail in the introductory paper for this special issue. The Scotia Sea contains high concentrations of macronutrients which never become depleted despite the seasonal occurrence of intense phytoplankton blooms driven by iron supplied from South Georgia. Throughout the study, we observed the decline of one such austral spring bloom. On the 17th of November, the beginning of the study, the bloom was at its peak with near surface Chl *a* concentration reaching 6.75 mg m^{-3}. Our time series then captured the decline of the bloom as indicated by the gradual reduction of near surface Chl *a* concentration to 1.58 mg m^{-3} on the last day of sampling the 12th of December (Henson et al., this issue).

3.2. | *POC concentrations*

The time evolution of POC concentrations is fully described by Giering et al. (this issue). Briefly, POC concentrations beneath the mixed layer generally decreased with depth, with the most rapid decrease observed in the upper mesopelagic (here 95–195 m depth: Fig. 3). In the mixed layer (upper 95 m), POC concentration revealed the typical temporal decline as expected from a declining spring phytoplankton bloom, decreasing from 252 mg C m^{-3} to 142 mg C m^{-3} at 0–10 m. In the (upper) mesopelagic, we initially observed an increase in POC concentrations at a daily rate of up to ~3% d^{-1} between 15 Nov and Dec 5, 2017. Towards the end of the cruise (9–15 Dec 2017), POC concentrations decreased at rates of up to −2.7% d^{-1}. POC concentrations at 190–200 m depth ranged from 24 to 40 mg C m^{-3}.

3.3. | *ambient leucine concentrations*

Concentrations of ambient leucine in the seawater followed similar trends to POC concentration, whereby they also generally decreased with depth but were apparently enriched at some depths in the mesopelagic during the period of downward POC flux (Fig. 3). The decline was particularly sharp over the transition from the mixed layer to the mesopelagic: mixed layer concentrations ranged from 0.438 nM; 0.184 ± 0.012 to 0.958 ± 0.094 nM with a mean of 0.438 nM, whereas mesopelagic ambient leucine ranged from 0.006 ± 0.002 to 0.173 ±

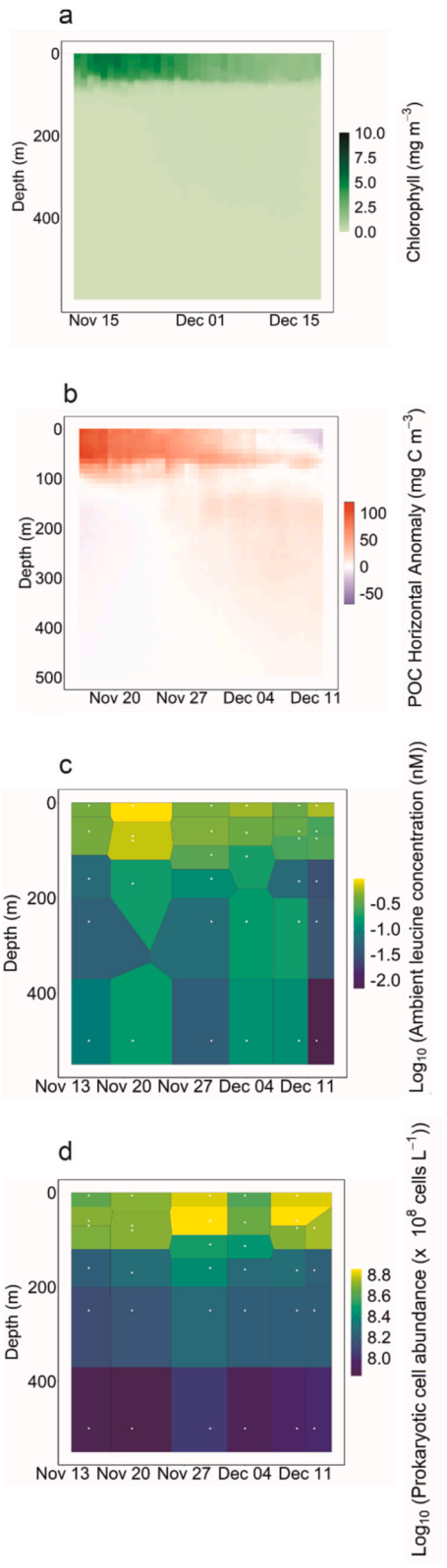

Fig. 3. The spatial and temporal dynamics of potential substrates over the surface mixed layer and mesopelagic to 500m during the COMICS expedition. (a) Glider-derived high-resolution concentrations of Chlorophyll *a* (b) Depth-specific anomalies (i.e. normalized to the mean of each depth). of particulate organic carbon (POC) based on high-resolution glider observations. (c) Concentrations of in situ leucine (bottle data), and (d) the abundance of prokaryotic cells (bottle data). White dots in panels c and d show sampling location for bottle data.

0.023 nM with a mean of 0.091 nM. The highest measured ambient leucine concentration coincided with the peak in POC concentration in November at 6 m and reached 252 mg C m^{-3} and 0.96 nM respectively. After this peak, we saw a decline in concentrations in the mixed layer during December with surface ambient leucine concentrations on the 12th of December having decreased to 0.27 nM as the bloom continued to dissipate and POC concentrations fell. It was noteworthy that at 500 m depth leucine was detected throughout the study, and prior to the downward flux of POC, with concentrations ranging from 0.007 to 0.160 nM at this depth.

3.4. prokaryotic abundance

Throughout the occupation of the study site, we observed the typical gradient in prokaryotic abundance (PA) over depth with concentrations in the upper mixed layer of mean, 5.10 x 10^5 cells mL^{-1}; 2.89–7.12 cells mL^{-1} compared to in the mesopelagic mean, 1.5 x 10^5 cells mL^{-1}; 6.79 x 10^4 - 2.60 x 10^5 cells mL^{-1} (Fig. 3). Rather than coinciding with peak POC and ambient leucine concentrations in early November, peaks in PA of 7.11 x 10^5 and 7.12 x 10^5 cells mL^{-1} occurred later at 60 m on the 30 Nov and the 10 Dec, respectively. PA decreased gradually with depth below 150 m at all stations, with the minima of 6.79 x 10^4 cells mL^{-1} observed at 500 m on the 21 Nov. In early December PA increased in the upper mesopelagic, although by the final cast cell numbers had reverted back to those observed at the start of the study.

3.5. | prokaryotic assimilation, respiration, and assimilation efficiency of leucine

Methodological differences in the way that rates of prokaryotic leucine respiration and leucine assimilation were measured were estimated to have caused an approximately 10% overestimation in the case of the former. However, this was a universal feature of the data set and was found to be independent of the concentration of background in situ leucine, and the therefore the varying degree of leucine elevation over the base line (data not shown). Therefore, it should be considered that our study systemically over estimated leucine respiration by approx 10%, and as a result LAE is systemically slightly underestimated. However, the general magnitudes of the respiration rates and LAE derived and their relative dynamics were robust.

Bulk ambient leucine assimilation rates were higher and more variable in the mixed layer (mean, 61.7 pmol L^{-1} h^{-1}; 7.67 ± 2.18–120.42 ± 0.94 pmol L^{-1} h^{-1}) than in the mesopelagic (mean, 1.96 pmol L^{-1} h^{-1}; 0.28 ± 0.07–12.90 ± 0.73 pmol L^{-1} h^{-1} (Fig. 4). The highest value of ambient leucine assimilation (120.42 ± 0.94 pmol L^{-1} h^{-1}) occurred at 63 m towards the end of the study on the 4 Dec. Leucine assimilation rates decreased rapidly between ~100 m and 150 m depth. Below ~150 m bulk leucine assimilation increased from the first occupation to a maximum of (12.90 ±

0.73 pmol L^{-1} h^{-1}) at 250 m on the 10 Dec. Data from the final time point showed that levels of bulk assimilation had reverted back to those observed at the start of the study.

Cell specific ambient leucine assimilation rates exhibited similar patterns to bulk ambient leucine assimilation rates with higher values in the mixed layer (mean, 1.14 X 10^{-7} pmol $cell^{-1}$ h^{-1}; 2.40 x 10^{-8} – 3.74 x 10^{-7} pmol $cell^{-1}$ h^{-1}) which decreased rapidly between 150 and 200 m. Cell specific ambient leucine assimilation rates in the mesopelagic varied between mean, 1.28 x 10^{-8}; 2.94 x 10^{-9} – 7.79 x 10^{-8} pmol $cell^{-1}$ h^{-1} and exhibited a similar temporal evolution in magnitude to bulk assimilation rates, increased throughout the study to a maximum at the penultimate time point before reverting to initial levels.

While bulk leucine respiration rates did not exhibit a pronounced variation over the study, cell-specific rates exhibited converse trends to the availability of potential substrates (as indicated by ambient leucine and POC concentrations) and leucine assimilation. Lowest rates were measured in the mixed layer and in the mesopelagic (250 m) per cell

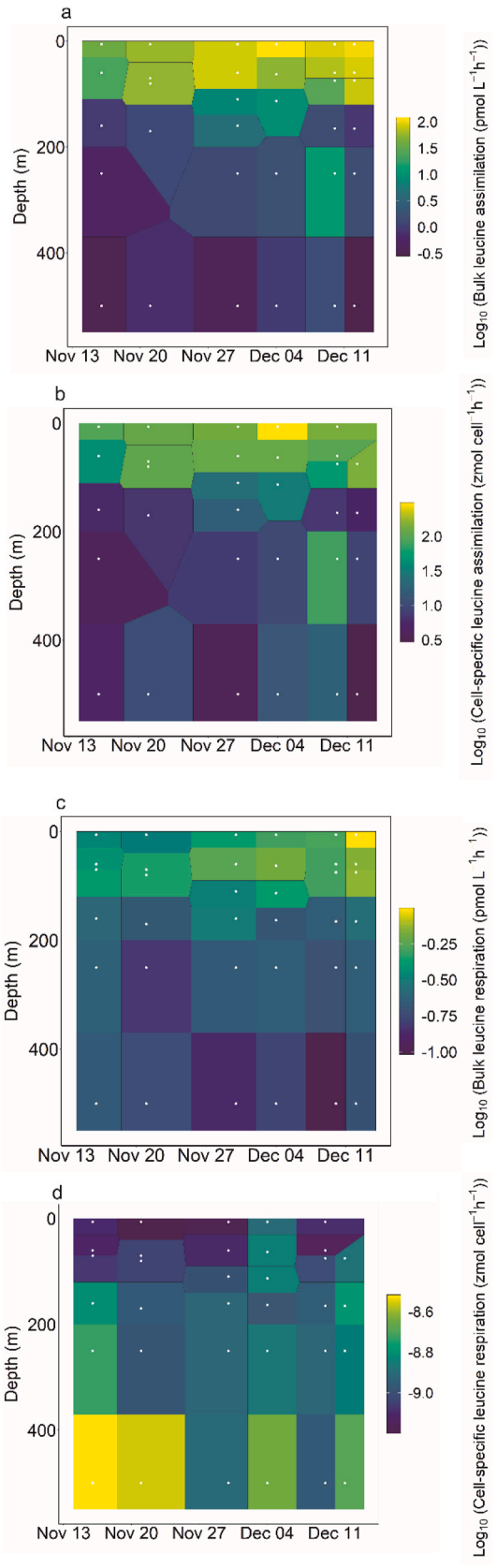

Fig. 4. The spatial and temporal dynamics of prokaryotic metabolism over the surface mixed layer and mesopelagic to 500m during the COMICS expedition in terms of (a) bulk in situ leucine assimilation rates, (b) cell-specific leucine assimilation rates, (c) bulk leucine respiration rates, and (d) cell-specific leucine respiration rates. White dots show sampling location for bottle data.

rates fell from 1.9 x 10^{-6} pmol cell^{-1} h^{-1} to 1.0 x 10^{-6} pmol cell^{-1} h^{-1} after the initial measurement and remained at this level until the final time point where they were observed to increase again.

LAE ranged from 0.58 to 0.99 over the water column (Fig. 5) with highest assimilation efficiency found in the surface mixed layer and lowest at depth. LAE in the mesopelagic was observed to generally increase over the study period although by the final cast at all depths below the mixed layer it had declined again, and particularly at 500 m where the lowest LAE of the study was recorded.

3.6. | *correlations of biogeochemical and metabolic data*

Over all depths surveyed concentrations of POC and ambient leucine were positively correlated with each other and to prokaryotic abundance, as well as to the bulk rates of leucine assimilation and respiration, cell specific rates of leucine assimilation and LAE (Fig. 6). However, rates of per cell leucine respired were negatively correlated to concentrations of both POC and ambient leucine, and they were also the strongest predictor of LAE. When examining the mixed layer in isolation, POC concentrations were a better predictor of prokaryotic abundance than ambient leucine concentrations, whereas in the mesopelagic this pattern was reversed. The primary predictor of leucine metabolism (anabolism v catabolism) between the two oceanic realms, was POC concentrations in the surface mixed layer, which were strongly negatively related to per cell leucine respiration rates, whereas in the mesopelagic ambient leucine concentrations related most significantly to per cell leucine assimilation rates. The best predictor of LAE was, in the mixed layer, rates of cell specific leucine assimilation, which were strongly positive, and in the mesopelagic, rates of cell specific leucine respiration, which were negative.

4. | discussion

In line with our hypothesis, the flux of POC from the mixed layer into the ocean's interior, driven by the Southern Ocean spring bloom collapse, was accompanied by a dynamic response in prokaryotic metabolic rates. As mesopelagic POC concentrations were enhanced, prokaryotic heterotrophic production (as indicated by leucine assimilation) was upregulated, per cell rates of leucine respiration were suppressed, and cell abundance increased. However, despite POC concentrations remaining elevated at depth, these shifts in the prokaryotic community were temporary and had already reverted, or begun to revert, within the study period. The observed dynamic prokaryote response could make balancing their consumption of C against the attenuation of POC flux challenging without temporal resolution. As prokaryotic consumption is the dominant process by which the downward flux of organic material is reduced or attenuated (Steinberg et al., 2008; Giering et al., 2014), these data build on the suggestion of (Herndl et al., 2022) that spatial measurement mismatches may account for the inability to balance the mesopelagic C budget (Burd et al., 2010; Steinberg et al., 2008). This highlights the importance of temporally resolved lagrangian studies to accurately constrain the efficiency of the BCP (Stange et al., 2017; Giering et al., 2017).

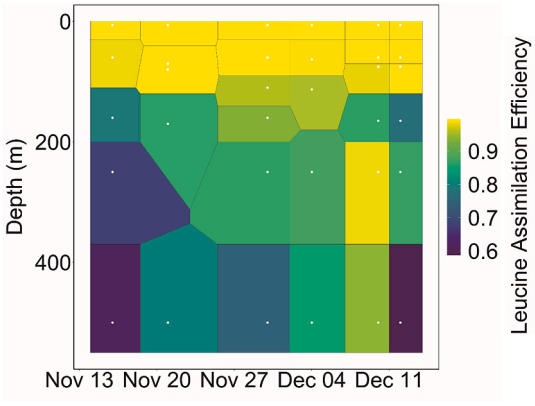

Fig. 5. The spatial and temporal dynamics leucine assimilation efficiency (LAE) over the surface mixed layer and mesopelagic to 500m during the COMICS expedition. White dots show sampling location for bottle data.

4.1. | *phasing of prokaryotic response to organic matter input*

The enhancement of mesopelagic prokaryotic growth rates and efficiency (as indicated by LAE; see section 4.2) in response to enrichment by sinking POC was already apparent from the first two time points of our study. When considering the implications of our findings it is pertinent to note that leucine uptake-based methods to determine prokaryotic metabolism, as we employed, likely yield rates which include contributions from both free-living and particle-associated prokaryotes (Schapira et al., 2012), although encountering particles is unusual given that they are rare. Thus, the response observed could be attributable to prokaryotes associated with the particles themselves, or those present in the water column, or a combination of both. Free-living microbes at depth are thought to maintain metabolic readiness so they may respond quickly to the influx of substrates (del Giorgio and Cole, 1998) which particles release to the dissolved phase. Sinking particles can also be rapidly colonized by prokaryotes according to factors such as motility, as this dramatically increases encounter rate, and allows otherwise rare microbes to be numerically dominant on particles (Lambert et al., 2019).

Elevation of prokaryotic metabolism was highest in the upper mesopelagic during the midpoint of our study, whereas deeper in the water column the peak came later implying a lag associated with the time required for the material to sink. An interesting feature of the data we gathered was that despite POC concentrations still being enriched at the final time point, prokaryotic abundance had already begun to decline. This could be attributable to the activity of mortality agents such as grazers or viruses (Evans and Brussaard, 2012; Ducklow and Carlson, 1992b; Gasol et al., 2002), which are more effective at prey capture/host infection under conditions of higher density and thus had, by this point, reached a threshold where they were able to crop down the prokaryotes faster than their multiplication. However, mortality would not account for the parallel reduction in mesopelagic prokaryotic growth and apparent growth efficiency that we also observed by the final time point.

It is possible that the reduction in mesopelagic prokaryotic metabolic rates observed at the last time point of the study could be accounted for by a reduction in substrate availability. Substrate lability may be driven by transformation and consumption of organic matter by prokaryotes (Pomeroy et al., 2007; Jiao et al., 2011; Dittmar et al., 2021) or, specifically with regards to particle associated communities, as a function of ecosystem capacity determined by prokaryotic composition and social behavior (Ebrahimi et al., 2019; Nguyen et al., 2022). Thus, potentially the prokaryotic community composition had shifted to one less favorable to consume the substrates available. Likely, another relevant factor is that particle sinking speeds are believed to dictate the composition of their associated microbial communities and the nature of organic substrates they supply via leaching to the dissolved phase (Wu et al., 2018; Ebrahimi et al., 2019; Nguyen et al., 2022). Villa-Alfageme and colleagues (this issue) found that particle sinking speeds were at their minimum during the final phase of the study. Hence reduced prokaryotic metabolic rates could be due to lower substrates concentrations in dissolved phase limiting free-living prokaryotic production. It is likely that the prokaryotic metabolic dynamics were the net result of multiple biotic and abiotic factors which lead to distinct phasing of the metabolic response over the export event.

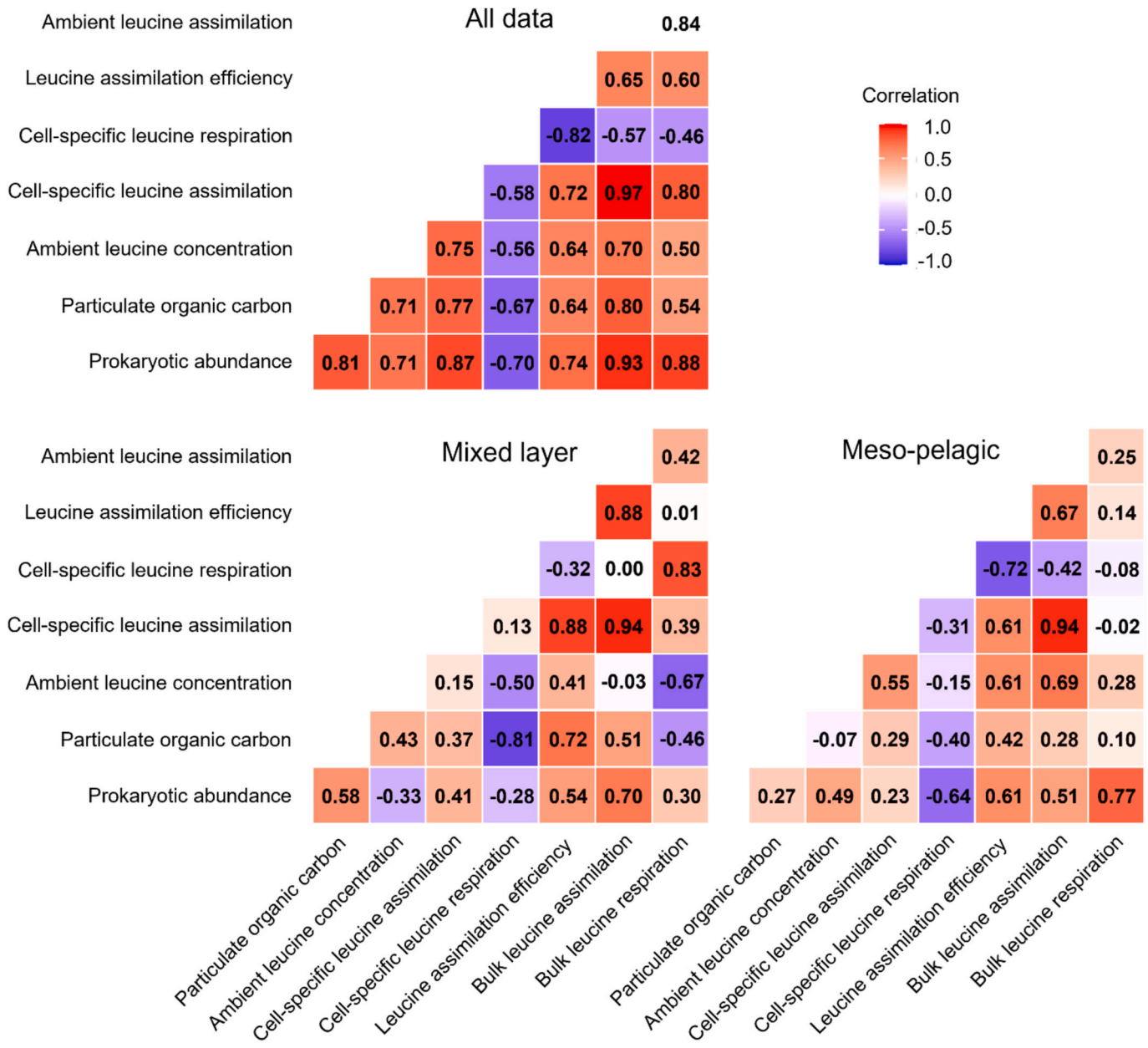

Fig. 6. Correlation matrices of potential substrates (POC and in situ leucine concentrations) prokaryotic abundance, and metabolism of leucine (specifically, the bulk and per cell rates of leucine assimilation and respiration and the Leucine assimilation efficiency) for all data, mixed layer only (0–95 m) and mesopelagic (depths >95 m). Numbers indicate the Pearson correlation coefficients (r) and the intensity of red or blue coloring the strength of the positive or negative correlation, respectively.

4.2. | prokaryotic ecophysiological shifts associated with the substrate regime

Through our study we consistently detected respiration of leucine by prokaryotes, in line with previous findings (Hobbie and Crawford, 1969; Suttle et al., 1991; Alonso-Sáez et al., 2007; Del Giorgio et al., 2011; Hill et al., 2013). This demonstrates that oceanic prokaryotes routinely use leucine for catabolism (Massey et al., 1976), despite it being an essential amino acid. Generally, under conditions of growth, it is energetically more efficient to preferentially channel leucine to protein anabolism over other metabolic pathways (del Giorgio and Cole, 1998; Díaz-Pérez et al., 2016). The observation that leucine is respired, and that this is consistently the case in marine prokaryotic communities, indicates (a) that, under typical oceanic conditions, achieving prokaryotic maintenance energy is dependent on the catabolism of a portion of leucine and, likely, other anabolically high-value substrates, and (b) that it is, therefore, likely a suitable molecule for use in indicating assimilation efficiency, and thus cellular metabolic status.

The metabolic fate of such substrates reflects the overall nature and availability of organic substrates and nutrients, as well as the physiological state and composition of the microbial community (Hollibaugh, 1994). Leucine metabolism has been applied as an index for both substrate processing and energy limitation, and, while not directly correlated, leucine assimilation efficiency (LAE) generally follows trends of PGE (Del Giorgio et al., 2011; Alonso-Sáez et al., 2007). Thus, constraining rates of leucine metabolism and LAE, in the context of potential substrates (POC and in situ leucine concentrations), provided insights into the ecophysiological shifts associated with the changing substrate regime during the export event.

When considering the water column as a whole, the positive

correlations between all measured variables, with the exception of cell specific leucine respiration rates (which were universally negatively related to the other parameters), confirmed the expected microbial response to the demise of the spring phytoplankton bloom. Specifically, that, as substrates increased, prokaryotic growth was stimulated, abundance increased and growth efficiency increased.

It follows then that the influx of substrates to the system relieved some form of resource-driven prokaryotic growth limitation, allowing cells to devote a greater proportion of leucine to growth relative to energy generation. Oceanic prokaryotes may be limited by nutrients (Rivkin and Anderson, 1997), the amount and the nature of the C supply (Carlson and Ducklow, 1996; Kähler et al., 1997; Cherrier and Bauer, 2004) or by energy (Carlson et al., 2007; van Wambeke et al., 2007), although it has been highlighted that the distinction between the latter two factors may be indistinguishable (del Giorgio and Cole, 1998).

Our findings indicated that the nature of prokaryotic resource limitation was likely distinct in the surface mixed layer compared with the underlying mesopelagic. As indicated by correlations, in the mixed layer, the concentration of in situ leucine did not seem to drive rates of its assimilation, rather POC concentration was a strong negative driver of cell specific leucine respiration (Fig. 6). This could indicate that POC supplied substrates relieved prokaryotic C-limitation. Thus, more leucine could be devoted to growth, coupling leucine assimilation to LAE, and thus also likely to PGE. Conversely, in the mesopelagic, in situ leucine concentrations appeared more significant in controlling prokaryote metabolism than POC concentration, and were more closely related to per cell leucine assimilation, than respiration. Our results also indicated that, in the mesopelagic, respiration was a stronger determinant of LAE then growth.

Amino acids have relatively high energy and C contents and they may release prokaryotes from limitation by both C and energy (del Giorgio and Cole, 1998). However, the stronger influence of leucine availability over bulk C, could be taken to imply stronger levels of energy limitation in the deeper ocean compared to the surface. Alternatively, the lower influence of POC concentration on prokaryotic metabolism in the mesopelagic then in the surface mixed layer could be due to changes in the composition of organic matter which made it less bioavailable (Pomeroy et al., 2007; Jiao et al., 2011). As this matter may have been already processed by prokaryotes after its production in the euphotic layer, its chemical nature may have been changed, consequently altering the energy yields, nutrients, and C precursors for biosynthesis for a given rate of bulk C consumption (Linton and Stephenson, 1978; del Giorgio and Cole, 1998).

Previous work has concluded that Southern Ocean prokaryotes are limited by both C and iron (Obernosterer et al., 2015), although the latter was shown not to be a factor during the COMICS study (Ainsworth et al., this issue). It is logical that energy could also limit Southern Ocean prokaryotes, and that this would be more pronounced in the mesopelagic, than in the surface ocean. This is likely given the strong seasonality at high latitudes meaning that prokaryotic communities would have to cope with variable organic matter inputs to the system. This could be exacerbated at depth where penetration of substrates might be far more episodic than in the surface ocean.

Thus, as with prokaryotes in oligotrophic waters (Ishida et al., 1986; del Giorgio and Cole, 1998) Southern Ocean prokaryotic populations may need a high energy flux in the cell in order transport solutes against large concentration gradients during periods of low organic matter inputs. During such periods, populations may also exist in a state of starvation survival with only minimum metabolism. Furthermore, under conditions of highly variable substrate supply, it has been postulated that cells maintain membrane energization, active transport systems and catabolic enzymes, so that they are able to respond rapidly when environmental conditions change (del Giorgio and Cole, 1998). Such factors have been previously cited to explain patterns of increasing energy limitation of prokaryotes from inshore to offshore, and from surface to deep in the Pacific (Del Giorgio et al., 2011).

4.3. | *labile substrate supply to the mesopelagic*

The detection of dissolved free amino acids at 500 m, the deepest depth we surveyed, during the initial measurements of our observation period could suggest that labile prokaryotic substrates are supplied to the mesopelagic via pathways other than downward POC flux. This is since these initial observations were prior to the arrival of the surface derived POC pulse that occurred during our study period. Although it should be noted that Henson et al. (this issue) reported that POC export events had already occurred at the site ahead of our study commencing. However, as the longest in situ leucine turnover time that we calculated for the mesopelagic was 9 days, and typically turnover was around 4 days, and the previous export events had happened two weeks prior to our study, this explanation is less probable.

Alternatively, deep convection may be responsible for enriching labile molecules in the mesopelagic (Backhaus et al., 2003) or autochthonous substrates may be supplied by the mortality of indigenous prokaryotes, and other organisms, via processes such as lysis by viruses (Wilhelm and Suttle, 1999) or predation by grazers (Johannes and Webb, 1965). If substrates are generated by the death of prokaryotes, which were formed by heterotrophic production, as opposed to chemoautotrophy (Middelburg, 2011), this cycle represents a closed trophic loop. Cycling of C within the mesopelagic is supported by the consistent detection of prokaryotic metabolism in the deep (Arístegui et al., 2005; Baltar et al., 2010; Gasol et al., 2009).

4.4. | *prokaryotic metabolism in different ocean regions and consequences for carbon cycling*

Underlying long-term 'base' energy supply and substrate quality and quantity likely accounted for the degree of prokaryotic energy and C limitation indicated by our measurements (see section 4.2). The more distal a prokaryote community is from the source of labile organic matter in the surface ocean or the coast, both spatially and temporally, the less substrate is typically available for metabolic processes and the quality of this substrate is likely lower. Specifically the drop in substrate quality, i.e. bioavailability, likely results from the more labile compounds having already been consumed (Hansell, 2013). Hence, 'distal' prokaryotic communities are likely to be pushed towards, not only C limitation, but also energy limitation (e.g. lack of vital micronutrients and organic compounds). Under energy limitation leucine, and other anabolically high value substrates, will be channeled towards catabolic processes in order to maintain basic cell functioning (rather than growth or reproduction), resulting in low assimilation efficiencies (see review by Giering and Evans, 2022) as was indicated by the low LAE we observed in the mesopelagic. Besides the quantity and quality, the consistency of substrate supply will have an influence on cell metabolic status and thus the degree of energy limitation. Under stable conditions, even when the amount of substrate may be low, cells are more likely to be adapted and not speculatively maintaining their membrane energization, or active transport systems and catabolic enzymes as has been postulated for starved communities (del Giorgio and Cole, 1998). Thus, the patterns of increasing energy limitation from inshore to offshore, and from surface to deep (del Giorgio et al., 2011; our study) can likely be further extrapolated to predict variations according to factors such as latitude and season (Fig. 7).

In tropical locations where productivity is high and subject to little variation during the most and least productive seasons, surface water prokaryotes could be assumed to have high growth efficiency, and not tend towards energy, or even C limitation, even during the lowest point in productivity during the year (Fig. 7a). Mesopelagic prokaryotes at such a tropical location (assuming a continuous downward flux of a fraction of surface derived POC) would have lower growth efficiency when compared with those in the surface waters owing to overall lower supply of substrate quality and quantity, given that they are spatially distal to the surface community. However, while tropical mesopelagic

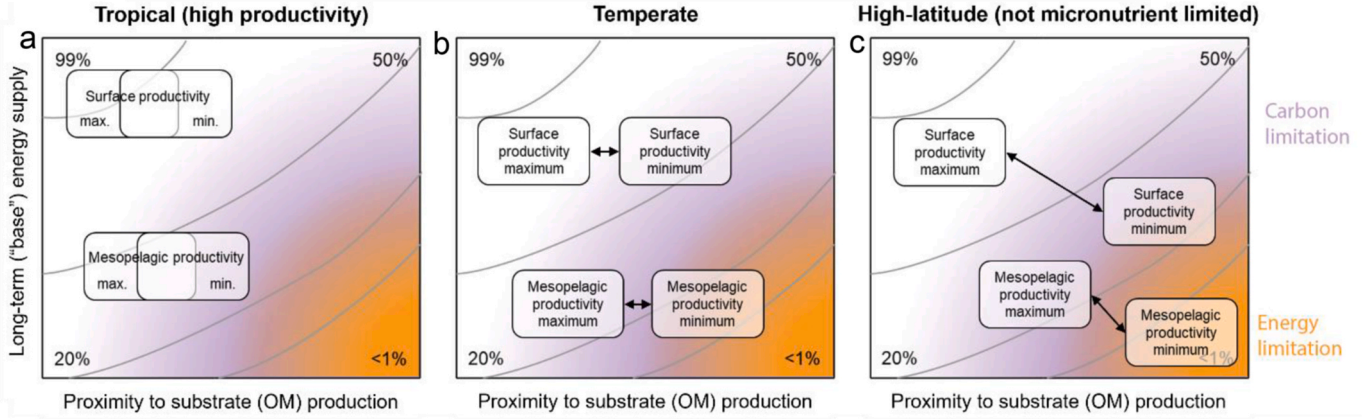

Fig. 7. Theoretical scheme indicating the influence of base energy supply (in terms of amount and stability of substrate) and proximity to substrate production (in terms of both depth and time) on prokaryotic growth efficiency. Speculative prokaryotic growth efficiencies projected for the extremes of the different substrate regime scenarios are given as percentages. Color intensities indicate the likely gradients in the degree of (purple) carbon limitation and (orange) energy limitation. The probable metabolic status of real-world prokaryotic communities within this scheme across different example ocean realms, and seasons according to maximum and minimum levels of system productivity, are indicated by the black outlined ovals.

prokaryotes might tend more towards C limitation then their surface counterparts, given that their substrate supply would be continuous owing to the less pronounced seasonal differences in productivity at the tropics, they would, in line with the surface community, be disinclined towards energy limitation. Conversely, in high latitude environments (assuming no micronutrient limitation, as with our study) where productivity varies substantially (from extremely high levels at the maximum to extremely low at the minimum levels through the year), surface communities in the productive season would likely have a high growth efficiency and low tendency to C and energy limitation but during the unproductive period, due to being temporally distal to organic matter supply they would be driven towards low growth efficiency and likely both C and energy limitation (Fig. 7c). For high latitude mesopelagic prokaryotes in the low productivity season, low growth efficiency, and C and energy limitation would be particularly acute given both their temporal and spatial distance from organic matter inputs. At mid latitude, temperate sites, given the intermediate levels of productivity and seasonality, 'baseline' supply would be expected to be lower and more consistent than at high latitudes and potentially higher but more seasonal than at the tropics (Fig. 7b). At such locations, patterns of prokaryotic growth efficiency, and C and energy limitation would be akin to high latitudes, but with less pronounced extremes.

Differences in prokaryotic communities' metabolic status throughout distinct ocean regions, resulting from distinctions in the quality, quantity and consistency of substrate supply, will have consequences for C cycling at those locations. The intensity of prokaryotic energy limitation influences the magnitude and efficiency of C assimilation, and thus, the amount of organic matter converted back to cellular biomass via secondary production (rather than back to dissolved inorganic C via respiration). Hence, the degree to which oceanic conditions promote prokaryotic energy limitation at a given ocean region will have consequences for the subsequent magnitude of the C flux through the microbial C loop (Pomeroy et al., 2007). As conditions of energy limitation favor respiration over assimilation of substrates (Harder, 1997; Russell and Cook, 1995; Stouthamer and Corry, 1973), it could be surmised that energetically limited prokaryotic communities in the mesopelagic would favor a weaker microbial loop (i.e. higher proportion of respiration to secondary production). Thus, over the course of our study the relative strength of the microbial loop is likely to have increased in the mesopelagic.

4.5. | conclusions

We demonstrated that the mesopelagic prokaryotic metabolic response to large scale export events is dynamic and responds quickly to increases in organic matter supply. Thus, the apparent efficiency of the BCP, as determined by prokaryotic activity, will vary according to the point at which it is measured. This infers that a time course of measurements throughout episodic export events is favorable to accurately constrain the efficiency of organic matter transfer to the deep, and thereby ocean carbon sequestration. A combination of abiotic and biotic factors is likely at play in controlling temporal shifts in prokaryotic metabolic rates with particle sinking speed likely a key factor. Furthermore, our findings indicated that energetically limited prokaryotic communities will respire a greater proportion of substrates compared with using them for production with implications for the strength of the microbial loop and thus carbon cycling.

CRediT authorship contribution statement

Rachel R.-P. Rayne: Formal analysis, Investigation, Writing – original draft, Writing – review & editing. **Sarah L.C. Giering:** Formal analysis, Investigation, Software, Supervision, Visualization, Writing – original draft, Writing – review & editing. **Manuela Hartmann:** Conceptualization, Funding acquisition, Methodology, Resources, Writing – review & editing. **Joost Brandsma:** Data curation, Formal analysis, Supervision, Visualization, Writing – review & editing. **Richard D. Sanders:** Conceptualization, Funding acquisition, Supervision, Writing – original draft. **Claire Evans:** Conceptualization, Formal analysis, Funding acquisition, Investigation, Methodology, Project administration, Supervision, Writing – original draft, Writing – review & editing.

Declaration of competing interest

The authors declare that they have no known competing financial interests or personal relationships that could have appeared to influence the work reported in this paper.

Data availability

Data will be made available on request.

Acknowledgements

We thank the scientists and crew of the DY086 expedition aboard RV Discovery. The Controls over Ocean Mesopelagic Interior Carbon Storage (COMICS) study was funded by a Large Grant from the United

Kingdom's Natural Environmental Research Council (NE/M020835/1) to RS. RR was supported by a SPITFIRE studentship. C.E. was supported by Natural Environment Research Council Independent Research Fellowship NE/M018806/1. We greatly thank Filipa Carvalho, Stephanie Henson and Nathan Briggs for providing glider data. We thank two anonymous reviewers whose feedback improved the quality of this manuscript.

References

Alonso-Sáez, L., Gasol, J.M., Arístegui, J., Vilas, J.C., Vaqué, D., Duarte, C.M., Agustí, S., 2007. Large-scale variability in surface bacterial carbon demand and growth efficiency in the subtropical northeast Atlantic Ocean. Limnol. Oceanogr. 52, 533–546.

Arístegui, J., Duarte, C.M., Gasol, J.M., Alonso-Sáez, L., 2005. Active mesopelagic prokaryotes support high respiration in the subtropical northeast Atlantic Ocean. Geophys. Res. Lett. 32.

Backhaus, J.O., Hegseth, E.N., Wehde, H., Irigoien, X., Hatten, K., Logemann, K., 2003. Convection and primary production in winter. Mar. Ecol. Prog. Ser. 251, 1–14.

Baltar, F., Arístegui, J., Gasol, J.M., Herndl, G.J., 2010. Prokaryotic carbon utilization in the dark ocean: growth efficiency, leucine-to-carbon conversion factors, and their relation. Aquat. Microb. Ecol. 60, 227–232.

Banse, K., 1994. Grazing and zooplankton production as key controls of phytoplankton production in the open ocean. Oceanography 7, 13–20.

Behrenfeld, M.J., Boss, E.S., 2014. Resurrecting the ecological underpinnings of ocean plankton blooms. Ann. Rev. Mar. Sci 6, 167–194.

Blain, S., Guieu, C., Claustre, H., Leblanc, K., Moutin, T., Quéguiner, B., Ras, J., Sarthou, G., 2004. Availability of iron and major nutrients for phytoplankton in the northeast Atlantic Ocean. Limnol. Oceanogr. 49, 2095–2104.

Boyd, P.W., Claustre, H., Levy, M., Siegel, D.A., Weber, T., 2019. Multi-faceted particle pumps drive carbon sequestration in the ocean. Nature 568, 327–335.

Briggs, N., Perry, M.J., Cetinić, I., Lee, C., D'asaro, E., Gray, A.M., Rehm, E., 2011. High-resolution observations of aggregate flux during a sub-polar North Atlantic spring bloom. Deep Sea Res. Oceanogr. Res. Pap. 58, 1031–1039.

Burd, A.B., Hansell, D.A., Steinberg, D.K., Anderson, T.R., Arístegui, J., Baltar, F., Beaupré, S.R., Buesseler, K.O., Dehairs, F., Jackson, G.A., Kadko, D.C., Koppelmann, R., Lampitt, R.S., Nagata, T., Reinthaler, T., Robinson, C., Robison, B. H., Tamburini, C., Tanaka, T., 2010. Assessing the apparent imbalance between geochemical and biochemical indicators of meso- and bathypelagic biological activity: what the @$♯! is wrong with present calculations of carbon budgets? Deep Sea Research Part Ii: Topical Studies in Oceanography 57, 1557–1571.

Carlson, C.A., Ducklow, H.W., 1996. Growth of bacterioplankton and consumption of dissolved organic carbon in the Sargasso Sea. Aquat. Microb. Ecol. 10, 69–85.

Carlson, C.A., Del Giorgio, P.A., Herndl, G.J., 2007. Microbes and the dissipation of energy and respiration: from cells to ecosystems. Oceanography 20, 89–100.

Cherrier, J., Bauer, J.E., 2004. Bacterial utilization of transient plankton-derived dissolved organic carbon and nitrogen inputs in surface ocean waters. Aquat. Microb. Ecol. 35, 229–241.

Cho, B.C., Azam, F., 1988. Major role of bacteria in biogeochemical fluxes in the ocean's interior. Nature 332, 441–443.

Conte, M.H., Ralph, N., Ross, E.H., 2001. Seasonal and interannual variability in deep ocean particle fluxes at the oceanic flux Program (Ofp)/Bermuda Atlantic time series (Bats) site in the western Sargasso Sea near Bermuda. Deep Sea Research Part Ii: Topical Studies in Oceanography 48, 1471–1505.

De Corte, D., Varela, M.M., Louro, A.M., Bercovici, S.K., Valencia-Vila, J., Sintes, E., Baltar, F., Rodríguez-Ramos, T., Simon, M., Bode, A., 2022. Zooplankton-derived dissolved organic matter composition and its bioavailability to natural prokaryotic communities. Limnol. Oceanogr.

Del Giorgio, P.A., Cole, J.J., 1998. Bacterial growth efficiency in natural aquatic systems. Annu. Rev. Ecol. Systemat. 29, 503–541.

Del Giorgio, P.A., Condon, R., Bouvier, T., Longnecker, K., Bouvier, C., Sherr, E., Gasol, J. M., 2011. Coherent patterns in bacterial growth, growth efficiency, and leucine metabolism along a northeastern Pacific inshore-offshore transect. Limnol. Oceanogr. 56, 1–16.

Díaz-Pérez, A.L., Díaz-Pérez, C., Campos-García, J., 2016. Bacterial l-leucine catabolism as a source of secondary metabolites. Rev. Environ. Sci. Biotechnol. 15, 1–29.

Dittmar, T., Lennartz, S.T., Buck-Wiese, H., Hansell, D.A., Santinelli, C., Vanni, C., Blasius, B., Hehemann, J.-H., 2021. Enigmatic persistence of dissolved organic matter in the ocean. Nat. Rev. Earth Environ. 2, 570–583.

Ducklow, H.W., Carlson, C.A., 1992. Oceanic bacterial production. In: Marshall, K.C. (Ed.), Advances in Microbial Ecology. Springer Us, Boston, Ma.

Ducklow, H., Kirchman, D., 2000. Microbial Ecology of the Oceans. *Bacteria production and Biomass in the Oceans*. Wiley-Liss Inc., New York, p. 85.

Ebrahimi, A., Schwartzman, J., Cordero, O.X., 2019. Cooperation and spatial self-organization determine rate and efficiency of particulate organic matter degradation in marine bacteria. Proc. Natl. Acad. Sci. USA 116, 23309–23316.

Eiler, A., Langenheder, S., Bertilsson, S., Tranvik, L.J., 2003. Heterotrophic bacterial growth efficiency and community structure at different natural organic carbon concentrations. Appl. Environ. Microbiol. 69, 3701–3709.

Eppley, R.W., Peterson, B.J., 1979. Particulate organic matter flux and planktonic new production in the deep ocean. Nature 282, 677–680.

Evans, C., Brussaard, C.P.D., 2012. Regional Variation in Lytic and Lysogenic Viral Infection in the Southern Ocean and its Contribution to Biogeochemical Cycling. Applied and Environmental Microbiology. Aem.01388-12.

Gasol, J.M., Pedrós-Alió, C., Vaqué, D., 2002. Regulation of bacterial assemblages in oligotrophic plankton systems: results from experimental and empirical approaches. Antonie Leeuwenhoek 81, 435–452.

Gasol, J.M., Alonso-Sáez, L., Vaqué, D., Baltar, F., Calleja, M.L., Duarte, C.M., Arístegui, J., 2009. Mesopelagic prokaryotic bulk and single-cell heterotrophic activity and community composition in the Nw Africa–Canary Islands coastal-transition zone. Prog. Oceanogr. 83, 189–196.

Giering, S.L.C., Evans, C., 2022. Overestimation of prokaryotic production by leucine incorporation—and how to avoid it. Limnol. Oceanogr. 67, 726–738.

Giering, S.L.C., Sanders, R., Lampitt, R.S., Anderson, T.R., Tamburini, C., Boutrif, M., Zubkov, M.V., Marsay, C.M., Henson, S.A., Saw, K., Cook, K., Mayor, D.J., 2014. Reconciliation of the carbon budget in the ocean's twilight zone. Nature 507, 480.

Giering, S.L., Sanders, R., Martin, A.P., Henson, S.A., Riley, J.S., Marsay, C.M., Johns, D. G., 2017. Particle flux in the oceans: challenging the steady state assumption. Global Biogeochem. Cycles 31, 159–171.

Hansell, D.A., 2013. Recalcitrant dissolved organic carbon fractions. Ann. Rev. Mar. Sci 5, 421–445.

Harder, J., 1997. Species-independent maintenance energy and natural population sizes. FEMS Microbiol. Ecol. 23, 39–44.

Herndl, G.J., Bayer, B., Baltar, F., Reinthaler, T., 2022. Prokaryotic Life in the Deep Ocean's water column. Ann. Rev. Mar. Sci 15.

Hill, P.G., Warwick, P.E., Zubkov, M.V., 2013. Low microbial respiration of leucine at ambient oceanic concentration in the mixed layer of the central Atlantic Ocean. Limnol. Oceanogr. 58, 1597–1604.

Hobbie, J.E., Crawford, C.C., 1969. Respiration corrections for bacterial uptake of dissolved organic compounds in natural waters. Limnol. Oceanogr. 14, 528–532.

Hollibaugh, J.T., 1994. Relationship between thymidine metabolism, bacterioplankton community metabolic capabilities, and sources of organic matter. Microb. Ecol. 28, 117–131.

Ishida, Y., Eguchi, M., Kadota, H., 1986. Existence of obligately oligotrophic bacteria as a dominant population in the SouthSouth China Sea and the West Pacific ocean. Mar. Ecol. Prog. Ser 30, 197–203.

Jiao, N., Herndl, G.J., Hansell, D.A., Benner, R., Kattner, G., Wilhelm, S.W., Kirchman, D. L., Weinbauer, M.G., Luo, T., Chen, F., Azam, F., 2011. The microbial carbon pump and the oceanic recalcitrant dissolved organic matter pool. Nat Rev Micro 9, 555, 555.

Johannes, R.E., Webb, K.L., 1965. Release of dissolved amino acids by marine zooplankton. Science 150, 76–77.

Kähler, P., Bjornsen, P.K., Lochte, K., Antia, A., 1997. Dissolved organic matter and its utilization by bacteria during spring in the Southern Ocean. Deep Sea Research Part Ii: Topical Studies in Oceanography 44, 341–353.

Kwon, E.Y., Primeau, F., Sarmiento, J.L., 2009. The impact of remineralization depth on the air–sea carbon balance. Nat. Geosci. 2, 630–635.

Lambert, B.S., Fernandez, V.I., Stocker, R., 2019. Motility drives bacterial encounter with particles responsible for carbon export throughout the ocean. Limnology and Oceanography Letters 4, 113–118.

Lampitt, R., Salter, I., De Cuevas, B., Hartman, S., Larkin, K., Pebody, C., 2010. Long-term variability of downward particle flux in the deep northeast Atlantic: Causes and trends. Deep Sea Research Part Ii: Topical Studies in Oceanography 57, 1346–1361.

Linton, J., Stephenson, R., 1978. A preliminary study on growth yields in relation to the carbon and energy content of various organic growth substrates. FEMS Microbiol. Lett. 3, 95–98.

Llort, J., Lévy, M., Sallée, J.-B., Tagliabue, A., 2015. Onset, intensification, and decline of phytoplankton blooms in the Southern Ocean. ICES J. Mar. Sci. 72, 1971–1984.

Maas, A.E., Liu, S., Bolaños, L.M., Widner, B., Parsons, R., Kujawinski, E.B., Blanco-Bercial, L., Carlson, C.A., 2020. Migratory zooplankton Excreta and its influence on prokaryotic communities. Front. Mar. Sci. 7.

Manganelli, M., Malfatti, F., Samo, T.J., Mitchell, B.G., Wang, H., Azam, F., 2009. Major role of microbes in carbon fluxes during austral winter in the Southern Drake Passage. PLoS One 4, e6941.

Marie, D., Partensky, F., Jacquet, S., Vaulot, D., 1997. Enumeration and cell cycle analysis of natural populations of marine picoplankton by flow cytometry using the nucleic acid stain Sybr Green I. Appl. Environ. Microbiol. 63, 186–193.

Massey, L.K., Sokatch, J.R., Conrad, R.S., 1976. Branched-chain amino acid catabolism in bacteria. Bacteriol. Rev. 40, 42–54.

Middelboe, M., 2000. Bacterial growth rate and marine Virus–host dynamics. Microb. Ecol. 40, 114–124.

Middelburg, J.J., 2011. Chemoautotrophy in the ocean. Geophys. Res. Lett. 38.

Nguyen, T.T.H., Zakem, E.J., Ebrahimi, A., Schwartzman, J., Caglar, T., Amarnath, K., Alcolombri, U., Peaudecerf, F.J., Hwa, T., Stocker, R., Cordero, O.X., Levine, N.M., 2022. Microbes contribute to setting the ocean carbon flux by altering the fate of sinking particulates. Nat. Commun. 13, 1657.

Nielsdóttir, M.C., Moore, C.M., Sanders, R., Hinz, D.J., Achterberg, E.P., 2009. Iron limitation of the postbloom phytoplankton communities in the Iceland Basin. Global Biogeochem. Cycles 23.

Obernosterer, I., Fourquez, M., Blain, S., 2015. Fe and C co-limitation of heterotrophic bacteria in the naturally fertilized region off the Kerguelen Islands. Biogeosciences 12, 1983–1992.

Pomeroy, L.R., Leb Williams, P.J., Azam, F., Hobbie, J.E., 2007. The microbial loop. Oceanography 20, 28–33.

Raghukumar, S., 2017. The marine environment and the role of fungi. In: Fungi in Coastal and Oceanic Marine Ecosystems: Marine Fungi. Springer International Publishing, Cham.

Reinthaler, T., Van Aken, H.M., Herndl, G.J., 2010. Major contribution of autotrophy to microbial carbon cycling in the deep North Atlantic's interior. Deep Sea Research Part Ii: Topical Studies in Oceanography 57, 1572–1580.
Rivkin, R.B., Anderson, M.R., 1997. Inorganic nutrient limitation of oceanic bacterioplankton. Limnol. Oceanogr. 42, 730–740.
Russell, J.B., Cook, G.M., 1995. Energetics of bacterial growth: balance of anabolic and catabolic reactions. Microbiol. Rev. 59, 48–62.
Schapira, M., Mcquaid, C.D., Froneman, P.W., 2012. Metabolism of free-living and particle-associated prokaryotes: consequences for carbon flux around a Southern Ocean archipelago. J. Mar. Syst. 90, 58–66.
Sebastián, M., Estrany, M., Ruiz-González, C., Forn, I., Sala, M.M., Gasol, J.M., Marrasé, C., 2019. High growth potential of long-term starved deep ocean opportunistic heterotrophic bacteria. Front. Microbiol. 10, 760.
Smith Jr, K.L., Ruhl, H.A., Huffard, C.L., Messié, M., Kahru, M., 2018. Episodic organic carbon fluxes from surface ocean to abyssal depths during long-term monitoring in Ne Pacific. Proc. Natl. Acad. Sci. USA 115, 12235–12240.
Stange, P., Bach, L.T., Le Moigne, F.A.C., Taucher, J., Boxhammer, T., Riebesell, U., 2017. Quantifying the time lag between organic matter production and export in the surface ocean: implications for estimates of export efficiency. Geophys. Res. Lett. 44, 268–276.
Steinberg, D.K., Van Mooy, B.A.S., Buesseler, K.O., Boyd, P.W., Kobari, T., Karl, D.M., 2008. Bacterial vs. zooplankton control of sinking particle flux in the ocean's twilight zone. Limnol. Oceanogr. 53, 1327–1338.
Stouthamer, A., Corry, B., 1973. Utilization of energy for growth and maintenance in continuous and batch cultures of microorganisms. Biochim. Biophys. Acta Rev. Bioenerg. 301, 53–70.
Suttle, C.A., Chan, A.M., Cottrell, M.T., 1990. Infection of phytoplankton by viruses and reduction of primary productivity. Nature 347, 467–469.
Suttle, C.A., Chan, A.M., Fuhrman, J.A., 1991. Dissolved free amino acids in the Sargasso Sea: uptake and respiration rates, turnover times, and concentrations. Mar. Ecol. Prog. Ser. 189–199.
Tang, K.W., Turk, V., Grossart, H.-P., 2010. Linkage between crustacean zooplankton and aquatic bacteria. Aquat. Microb. Ecol. 61, 261–277.
Vallino, J.J., Hopkinson, C.S., Hobbie, J.E., 1996. Modeling bacterial utilization of dissolved organic matter: Optimization replaces Monod growth kinetics. Limnol. Oceanogr. 41, 1591–1609.
Van Wambeke, F., Obernosterer, I., Moutin, T., Duhamel, S., Ulloa, O., Claustre, H., 2007. Heterotrophic bacterial production in the South East Pacific: longitudinal trends and coupling with primary production. Biogeosci. Discuss. 4, 2761–2791.
Volk, T., Hoffert, M.I., 1985. Ocean carbon pumps: analysis of relative strengths and efficiencies in ocean-driven atmospheric Co2 changes. The carbon cycle and atmospheric Co2: natural variations Archean to present 32, 99–110.
Wikner, J., Hagström, Å., 1988. Evidence for a tightly coupled nanoplanktonic predator-prey link regulating the bacterivores in the marine environment. Mar. Ecol. Prog. Ser. 50, 137–145.
Wilhelm, S.W., Suttle, C.A., 1999. Viruses and Nutrient Cycles in the Sea: viruses play critical roles in the structure and function of aquatic food webs. Bioscience 49, 781–788.
Wright, R.R., Hobbie, J.E., 1966. Use of Glucose and Acetate by bacteria and Algae in aquatic ecosystems. Ecology 47, 447–464.
Wu, X., Wu, L., Liu, Y., Zhang, P., Li, Q., Zhou, J., Hess, N.J., Hazen, T.C., Yang, W., Chakraborty, R., 2018. Microbial interactions with dissolved organic matter drive carbon dynamics and community succession. Front. Microbiol. 9.
Zubkov, M.V., Burkill, P.H., 2006. Syringe pumped high speed flow cytometry of oceanic phytoplankton. Cytometry Part A: The Journal of the International Society for Analytical Cytology 69, 1010–1019.
Zubkov, M.V., Tarran, G.A., Mary, I., Fuchs, B.M., 2007. Differential microbial uptake of dissolved amino acids and amino sugars in surface waters of the Atlantic Ocean. J. Plankton Res. 30, 211–220.